The Journal of Chemical Physics

ELECTRODE: An electrochemistry package for atomistic simulations

Cite as: J. Chem. Phys. **157**, 084801 (2022); https://doi.org/10.1063/5.0099239
Submitted: 16 May 2022 • Accepted: 25 July 2022 • Accepted Manuscript Online: 25 July 2022 • Published Online: 25 August 2022

Ludwig J. V. Ahrens-Iwers, Mathijs Janssen, Shern R. Tee, et al.

The Journal of Chemical Physics ARTICLE scitation.org/journal/jcp

ELECTRODE: An electrochemistry package for atomistic simulations

Cite as: J. Chem. Phys. 157, 084801 (2022); doi: 10.1063/5.0099239
Submitted: 16 May 2022 • Accepted: 25 July 2022 •
Published Online: 25 August 2022

Ludwig J. V. Ahrens-Iwers,[1] Mathijs Janssen,[2] Shern R. Tee,[3,a)] and Robert H. Meißner[4,5,b)]

AFFILIATIONS

[1] Institute of Advanced Ceramics, Hamburg University of Technology, Hamburg, Germany
[2] Mechanics Division, Department of Mathematics, University of Oslo, N-0851 Oslo, Norway
[3] Australian Institute for Bioengineering and Nanotechnology, The University of Queensland, Brisbane, Queensland, Australia
[4] Institute of Polymers and Composites, Hamburg University of Technology, Hamburg, Germany
[5] Helmholtz-Zentrum Hereon, Institute of Surface Science, Geesthacht, Germany

[a)] **Electronic mail:** s.tee@uq.edu.au
[b)] **Author to whom correspondence should be addressed:** robert.meissner@tuhh.de

ABSTRACT

Constant potential methods (CPMs) enable computationally efficient simulations of the solid–liquid interface at conducting electrodes in molecular dynamics. They have been successfully used, for example, to realistically model the behavior of ionic liquids or water-in-salt electrolytes in supercapacitors and batteries. CPMs model conductive electrodes by updating charges of individual electrode atoms according to the applied electric potential and the (time-dependent) local electrolyte structure. Here, we present a feature-rich CPM implementation, called ELECTRODE, for the Large-scale Atomic/Molecular Massively Parallel Simulator, which includes a constrained charge method and a thermo-potentiostat. The ELECTRODE package also contains a finite-field approach, multiple corrections for nonperiodic boundary conditions of the particle–particle particle–mesh solver, and a Thomas–Fermi model for using nonideal metals as electrodes. We demonstrate the capabilities of this implementation for a parallel-plate electrical double-layer capacitor, for which we have investigated the charging times with the different implemented methods and found an interesting relationship between water and ionic dipole relaxations. To prove the validity of the one-dimensional correction for the long-range electrostatics, we estimated the vacuum capacitance of two coaxial carbon nanotubes and compared it to structureless cylinders, for which an analytical expression exists. In summary, the ELECTRODE package enables efficient electrochemical simulations using state-of-the-art methods, allowing one to simulate even heterogeneous electrodes. Moreover, it allows unveiling more rigorously how electrode curvature affects the capacitance with the one-dimensional correction.

I. INTRODUCTION

A common approach to treat electrodes in atomistic simulations is to assume them to be uniformly charged walls, either structureless or atomically resolved. In the case of equilibrium electrolytes near planar electrodes at low charge densities, this approach is known to capture the electrochemical properties well. Several studies, however, have emphasized the importance of polarization of electrodes by the ions and molecules in their vicinity.[1–5] In more realistic electrochemical scenarios, constant potential method (CPM) molecular dynamics (MD) results are often significantly different from those obtained with uniformly charged electrodes.[6]

While the CPM[7,8] is a popular tool for modeling metal electrodes by dynamically updating individual charges on electrode atoms, alternatives such as image charge methods[9–12] are commonly used to enforce a constant potential for planar electrodes. While one of these methods can handle nonplanar surfaces by inducing a charge density on the interface between two media, most of them are limited to planar electrodes.[12] Those approaches faithfully reproduce the behavior of electrolytes near electrodes, particularly

the correlation between thermal fluctuations in the electrolyte near the electrode and the induced-charge polarization of the electrode, while obtaining a realistic picture of the electrical double-layer. A CPM MD simulation is able to capture the temporal response in the buildup and breakdown of electric double-layer and, thereby, allows realistic capacitor charging and discharging curves to be generated *in silico*.[6,13–15] Interestingly, near highly charged planar electrodes[16–18] and nonplanar electrodes (such as curved substrates or nanoporous carbons),[6,19–25] CPM MD and Monte Carlo simulations[26] yield a spatially specific charge polarization and a nontrivial electrolyte structure.

Here, we present a package for treating electrodes in MD simulations that interfaces with the Large-scale Atomic/Molecular Massively Parallel Simulator (LAMMPS).[27] Our ELECTRODE package uses the highly parallelized and efficient computational infrastructure of LAMMPS and allows interaction with many other packages and features already available in LAMMPS. This work builds, in part, on an earlier work in which we showed how a particle–particle particle–mesh (P^3M)-based calculation makes the electrostatic calculations of a CPM simulation more efficient.[28] In addition to some new improvements to the CPM, this implementation provides a constrained charge method (CCM) and a thermo-potentiostat (TP).[29] To capture the electronic response of nonideal metals, a Thomas–Fermi (TF) model[30] is included. Both an Ewald and a P^3M **k**-space solver are available for various constraints of periodicity of the systems, such as infinite slabs, cylinders, or fully 3D periodic systems. The ELECTRODE package also contains the closely related finite field (FF)[31] and finite displacement (FD)[32] methods, which extend CPM MD with a slab geometry to fully periodic boundary conditions for increased computational efficiency.[33]

A list of features in the ELECTRODE package is presented in Sec. II, including a brief description of their theoretical background. In Sec. III, we summarize the concept of CPM MD using data from various CPM MD runs and rationalize it based on the charging times of an electrical double-layer capacitor. We discuss briefly for which situation each approach is suitable and give an overview of future development directions and possible applications in Sec. IV.

II. FEATURES

A. Constant potential method

In atomistic electrochemical simulations, the system of interest is often a fluid electrolyte confined between two electrodes (cf. inset of Fig. 2). This could serve as an *in silico* nanoscale model of a capacitor, to optimize some metric, such as energy or power density, by modifying the electrolyte composition or electrode structure.

The distinctive feature of CPM MD is the calculation of electrode charges keeping electrodes at a desired electrostatic potential. To achieve this, we first partition the potential energy, U, of an MD simulation as follows:

$$U = U_{\text{non-Coul}} + U_{\text{elyt}} + U_{\text{elec}}. \tag{1}$$

Here, $U_{\text{non-Coul}}$ includes all non-Coulombic interactions, U_{elyt} includes all Coulombic interactions between electrolyte particles, and U_{elec} includes all Coulombic interactions involving electrode particles (both with electrolyte particles, and with other electrode particles). While the former are treated with regular force field approaches, the last term is given a somewhat special treatment. U_{elec}, i.e., without electrolyte–electrolyte interactions, is written in terms of an electrode charge vector $\mathbf{q}$ comprising all electrode charges as

$$U_{\text{elec}}(\{\mathbf{r}\},\mathbf{q}) = \frac{1}{2}\mathbf{q}^{\mathrm{T}}\mathbf{A}\mathbf{q} - \mathbf{b}^{\mathrm{T}}(\{\mathbf{r}\})\mathbf{q} - \mathbf{v}^{\mathrm{T}}\mathbf{q}, \tag{2}$$

with a matrix $\mathbf{A}$, and vectors $\mathbf{b}$ and $\mathbf{v}$, where $\mathbf{b}$ depends on the electrolyte positions $\{\mathbf{r}\}$. The applied potential $\mathbf{v}$ has an entry for every electrode atom. The interactions between electrode atoms are represented by $\mathbf{A}$, called elastance matrix due to the analogy between a vacuum capacitor and a spring. If the electrode atoms do not move, $\mathbf{A}$ can be precomputed, allowing significant computational savings. The electrolyte vector $\mathbf{b}(\{\mathbf{r}\})$ represents the electrostatic potential on each electrode atom due to the electrolyte atoms.

At each step, $\mathbf{q}$ is updated to minimize the Coulombic energy contribution U_{elec}, possibly subject to additional constraints. The desired energy-minimizing charge vector $\mathbf{q}^*$ is straightforward to calculate,[34]

$$\mathbf{q}^* = \mathbf{A}^{-1}[\mathbf{b}(\{\mathbf{r}\}) + \mathbf{v}]. \tag{3}$$

Here, the elastance has been inverted to yield $\mathbf{A}^{-1}$, which is called the capacitance matrix in light of its role in Eq. (3): The response of the charge vector $\mathbf{q}^*$ can calculated as the product of the capacitance matrix with the vector of external potentials, analogously to the well-known scalar equation $Q = CV$ linking the capacitance C to the charge Q.

Provided that the electrode atom positions and, thus, the vacuum capacitance are constant, the main computational burden is the calculation of $\mathbf{b}(\{\mathbf{r}\})$ at every time step, which is necessary due to the motion of the electrolyte. The primary purpose of ELECTRODE is to compute the electrode–electrolyte interaction in $\mathbf{b}$ efficiently and to update the electrode charges accordingly. Alternatively, the electrode charges could be obtained with the conjugate gradient method, which solves the minimization problem without matrix inversion.[35,36] Yet another approach is to treat the electrode charges as additional coordinates and perform mass-zero constrained dynamics for them.[37]

In MD with periodic boundary conditions, the simulation cell ideally is charge neutral. Scalfi *et al.*[34] showed that this constraint could be imposed by using the symmetric matrix

$$\mathbf{S} \equiv \mathbf{A}^{-1} - \frac{\mathbf{A}^{-1}\mathbf{e}\mathbf{e}^{\mathrm{T}}\mathbf{A}^{-1}}{\mathbf{e}^{\mathrm{T}}\mathbf{A}^{-1}\mathbf{e}}, \quad \mathbf{e}^{\mathrm{T}} = (1,\ldots,1) \tag{4}$$

as capacitance matrix instead of $\mathbf{A}^{-1}$.

Nonideal metallic electrodes have been recently modeled by Scalfi *et al.*[30] using a semiclassical TF approach. We have implemented this promising approach in our ELECTRODE package, as its implementation is very similar to the self-interaction correction of the Ewald summation[38] and contains only a single summation over the electrode atoms. An interesting alternative to effectively model a wide range of materials between insulator and ideal metal

was proposed by Schlaich *et al.*[39] and involved using a virtual TF fluid within the electrodes. However, the virtual TF fluid approach appears computationally more expensive. Both models require free parameters, most crucially the TF length, l_{TF}, in Scalfi *et al.*[30] and (a rather artificial) parameterization of the virtual TF fluid in the approach of Schlaich *et al.*[39] Further, assumptions such as atom-centered densities prohibit effects such as quantum spillover and delocalization of the image plane. It should be noted that ELECTRODE provides a more flexible implementation of the TF model, allowing heterogeneous electrodes with different l_{TF} for different atom types. For more general information on CPM MD approaches, the interested reader is referred to the excellent and thorough review of current electrode–electrolyte simulations by Scalfi *et al.*,[40] the well-written theory part of *MetalWalls*,[41] or the thesis of Gingrich.[42]

B. Simulating an arbitrary number of electrodes

A CPM MD simulation is typically performed with two electrodes, which means there are only two possible values for each of the n components of the potential in Eq. (2). In the ELECTRODE package, an arbitrary number N of electrodes is allowed with every electrode atom belonging to exactly one electrode. We define an electrode-wise indicator vector $\mathbf{g}_\alpha$ for every electrode α with n entries, which are equal to 1 if the respective electrode particle belongs to that electrode and 0 otherwise. The indicator matrix

$$\mathbf{G} = \begin{bmatrix} \mathbf{g}_1 & \mathbf{g}_2 & \cdots & \mathbf{g}_N \end{bmatrix} \tag{5}$$

comprising the indicator vectors of all N electrodes allows us to connect electrode-wise quantities to particle-wise quantities. From hereon, we use tildes for electrode-wise quantities. For instance, we define $\tilde{\mathbf{v}}$ as the electrode-wise potential and use it to write the potential $\mathbf{v} = \mathbf{G}\tilde{\mathbf{v}}$. Likewise, energy-minimizing charges $\mathbf{q}^*$ for a given set of electrode-potentials are

$$\mathbf{q}^* = \mathbf{S}(\mathbf{b} + \mathbf{v}) = \mathbf{S}\mathbf{b} + \mathbf{S}\mathbf{G}\tilde{\mathbf{v}}. \tag{6}$$

C. Simulating electrodes at specified total charge

In the CCM, the user sets the electrode-wise total charge $\tilde{\mathbf{q}}^*$ for each electrode. Such a fixed-charge setup corresponds to an open-circuit configuration.[43] This type of simulation has recently been attempted as a variation of the finite-field method.[32] Therein, it was found that ramping the total charge up or down over time could be considered computational amperometry, and a faster nonequilibrium response was observed.

Working with the capacitance matrix $\mathbf{A}^{-1}$ rather than the symmetrized matrix $\mathbf{S}$ (since charge neutrality is explicitly enforced by the appropriate choice of $\tilde{\mathbf{q}}^*$), we have the following:

$$\tilde{\mathbf{q}}^* = \mathbf{G}^{\mathrm{T}}\mathbf{q}^* = \mathbf{G}^{\mathrm{T}}\mathbf{A}^{-1}\mathbf{b} + \mathbf{G}^{\mathrm{T}}\mathbf{A}^{-1}\mathbf{G}\tilde{\mathbf{v}} \equiv \tilde{\mathbf{q}}_b^* + \tilde{\mathbf{C}}\tilde{\mathbf{v}}. \tag{7}$$

$\tilde{\mathbf{q}}_b^*$ defines the total charge each electrode would carry at zero potential and $\tilde{\mathbf{C}}$ is the electrode-wise capacitance matrix. To subsequently estimate $\tilde{\mathbf{q}}_b^*$, Eq. (7) is solved for $\tilde{\mathbf{v}}$, which is then applied using the CPM. This results in an energy minimization with respect to the charge distribution with a constraint on the total electrode charges. Analogous to how constant volume and constant pressure simulations can be thermodynamically equivalent, CCM and CPM simulations will give the same capacitances under suitable conditions. However, a thorough proof of that assertion is out of scope of this work and will be discussed in an upcoming work.

D. Simulating electrodes with a thermo-potentiostat

Deißenbeck *et al.*[29] recently presented a thermo-potentiostat (TP) that takes into account the fluctuation–dissipation relation of electrode charges at a given voltage and temperature in an electronic circuit. They have also provided a TP implementation based on a uniform charge distribution using the scripting capability of LAMMPS.[27] The ELECTRODE package provides an implementation that minimizes the energy with respect to the charge distribution and conforms to the formalism described by Deißenbeck *et al.*[29] Our TP approach is currently limited to only two electrodes, and instead of a vector of applied potentials $\tilde{\mathbf{v}}$, a potential difference

$$\Delta v_0 = v_{\mathrm{top}} - v_{\mathrm{bot}} \tag{8}$$

between two electrodes is used. At every time step, the potential difference $\Delta v(t)$ between the two electrodes is evaluated to find the new capacitor charge according to

$$q(t + \Delta t) = q(t) - C_0\left[\Delta v(t) - \Delta v_0\right]\left(1 - \mathrm{e}^{-\Delta t/\tau_v}\right) + X\sqrt{k_{\mathrm{B}} T_v C_0\left(1 - \mathrm{e}^{-2\Delta t/\tau_v}\right)}. \tag{9}$$

Here, k_{B} is the Boltzmann constant, τ_v and T_v are parameters of the TP, and X is a normally distributed random number with a mean of 0 and a standard deviation of 1. The vacuum capacitance C_0 is obtained from the capacitance matrix[34] and the effective potential $\Delta v(t)$ is computed from the electrode charges and the electrolyte configuration [cf. Eq. (7)]. Hence, all quantities required to evaluate Eq. (9) are readily available in the CPM. The obtained capacitor charge $\pm q(t + \Delta t)$ is applied using the CCM on both electrodes, respectively.

E. Simulations with different periodicity

The Ewald summation commonly assumes periodic boundary conditions in all three directions and has to be modified for systems with slab and one-dimensional periodic geometries. As shown by Smith,[44] a regular 3D Ewald summation for slab-like systems, which are periodic in the xy-plane but confined in the z-direction, results in a dipole term,

$$J^{2\mathrm{D}}(\mathbf{M}) = \frac{2\pi}{V} M_z^2. \tag{10}$$

Here, M_z is the z-component of the dipole of the simulation cell. This dipole term was subsequently used for correcting the infinite boundary artifact of slab-like systems.[45] This is known as the EW3Dc method, which is implemented in many MD codes including

LAMMPS.[27] Several authors[38,46–48] have shown that the infinite boundary contribution in slab-like geometries can also be solved in an exact form. This rarely implemented EW2D solver is another cornerstone of the ELECTRODE package.

Just like slab-like geometries, systems with only one periodic dimension require an appropriate treatment of the long-range electrostatic interactions. As shown by Bródka and Śliwiński,[49] the approach of Smith[44] can be generalized for an infinitely extended one-dimensional summation,

$$J^{1D}(\mathbf{M}) = \frac{\pi}{V}\left(M_x^2 + M_y^2\right). \tag{11}$$

Here, z is the periodic dimension and M_x and M_y are the respective components of the total dipole of the unit cell. Contrasting established codes, the ELECTRODE package contains these corrections for one-dimensional periodic systems. Even more crucially, ELECTRODE is the first package (as far as we know) to implement these corrections in combination with a CPM. As an outlook, the electrostatic layer correction[50] in combination with P^{3}M[51] is also considered for implementation as an alternative to the EW3Dc approach.

As illustrated for slab-like two-dimensional periodic systems, the boundary corrections can be easily incorporated into the CPM formalism by splitting the dipole components into their electrode and electrolyte contributions,

$$\begin{aligned} J^{2D} &= \frac{2\pi}{V}\left[\left(M_z^{\text{elec}}\right)^2 + 2M_z^{\text{elec}}M_z^{\text{elyt}} + \left(M_z^{\text{elyt}}\right)^2\right] \\ &= \frac{2\pi}{V}\left[\sum_{ij} z_i z_j q_i q_j + 2M_z^{\text{elyt}}\sum_i z_i q_i + \left(M_z^{\text{elyt}}\right)^2\right]. \end{aligned} \tag{12}$$

This way, dipole corrections fit into the linear form of the Coulombic energy in Eq. (2) that is used in the CPM and the computational effort for the electrode–electrolyte interaction scales linearly with the number of particles.

F. Simulating electrodes with the finite field method

In the FF method,[31] the potential difference between two electrodes is not directly specified using the applied potential $\mathbf{v}$. Instead, the simulation cell is periodic in the z-direction, i.e., without adding the artificial vacuum between the slabs required otherwise. The FF method allows efficient simulations of infinite electrode slabs, since no additional vacuum is required. However, electrodes with complex shapes or electrodes with one-dimensional periodicity cannot be simulated with the FF method.

A potential difference Δv_0 [cf. Eq. (8)] is created in the FF method by introducing a z-directed electric (polarization) field of magnitude $-\Delta v_0/L_z$, creating a discontinuity of Δv_0 across the periodic z-boundary (and thus between the two electrodes on either side of the slab). In this formulation, the electrode Coulombic energy is

$$U_{\text{elec}} = \frac{1}{2}\mathbf{q}^{\mathrm{T}}\mathbf{A}\mathbf{q} - \mathbf{b}^{\mathrm{T}}(\{\mathbf{r}\})\mathbf{q} + \Delta v_0 \boldsymbol{\zeta}^{\mathrm{T}}\mathbf{q}. \tag{13}$$

Here, $\boldsymbol{\zeta}$ is a vector containing the normalized z-positions of each electrode atom, viz., $\{\mathbf{z}/L_z\}$ with an offset for the bottom electrode to make the system symmetric along the z-direction, replicating the conductor-centered supercell in Ref. 31. The energy-minimizing charge $\mathbf{q}^*$ in this model is

$$\mathbf{q}^* = \mathbf{S}[\mathbf{b}(\{\mathbf{r}\}) - \Delta v_0 \boldsymbol{\zeta}], \tag{14}$$

which is equivalent to that obtained from the standard CPM, replacing $\mathbf{v}$ with $-\Delta v_0 \boldsymbol{\zeta}$.

III. RESULTS AND DISCUSSION

A. Charging times

A simple capacitor model is adapted from an example in the *MetalWalls* repository[52] and comprises a saline solution between two gold electrodes with three layers each. To compare the equilibrium conditions of the CPM and CCM, we calculated the capacitance per area from the averaged equilibrium charges and voltages at an applied voltage of 2 V and charge of 4.4e, respectively. The obtained values of 2.94 and 2.91 μF cm^{-2} for the CPM and CCM, respectively, differ by only 1%, showing good agreement between the methods at equilibrium.

When a voltage is initially applied with the CPM, the charge induced on both electrodes is very small since the capacitance of the electrode pair *in vacuo* is small.[28,34] However, the electrode charges induce the formation of a dipole in the electrolyte, which, in turn, induces additional charge on the electrode. CPM MD, thus, models the process of charging an electrical double layer capacitor physically correctly, and the charging–discharging curves obtained from CPM MD can be used to fit parameters for equivalent macroscopic electrical circuits.[53] Two charging times τ_1 and τ_2 are obtained by fitting a bi-exponential charging function given by

$$M_z(t) = M_z^{\text{eq}}\left[1 - c\,\exp(-t/\tau_1) - (1-c)\exp(-t/\tau_2)\right] \tag{15}$$

to the z-component of the electrolyte dipole.[54] M_z^{eq} is the extrapolated equilibrium dipole reached at late times. Comparing the individual contributions to the total electrolytic dipole reveals that τ_1 describes relatively fast water dipole relaxations and τ_2 describes charging times related to ion diffusion. To validate this statement, we show both individual components in Fig. 1. From the mixing parameters c in the panels, it is clear that water dipole relaxation dominates at the beginning, while ion diffusion prevails at later times. τ_1 of the water in Fig. 1(b) largely corresponds to that of the total dipole at the beginning of the charging. While the ions in Fig. 1(c) relax mainly on the slower timescale of τ_2, the water dipole decreases as the ion dipole is slowly built up.

Figure 2 compares results using CPM, CCM, and TP, the latter with a time constant τ_v = 100 fs, to each other and to their uniformly charged counterparts. We focus on the charging term with the faster timescale τ_1 because of its large contribution to the total dipole. For the uniform variants, the charges are always evenly distributed across the inner layers of the electrodes. The uniform methods are in general very close to their heterogeneous counterparts, which is consistent with previous studies that found only small differences between a heterogeneous and uniform CPM at low voltages for simple planar electrodes.[16] The charging times obtained with CCM appear to be too fast, since τ_1 is about two orders of magnitude

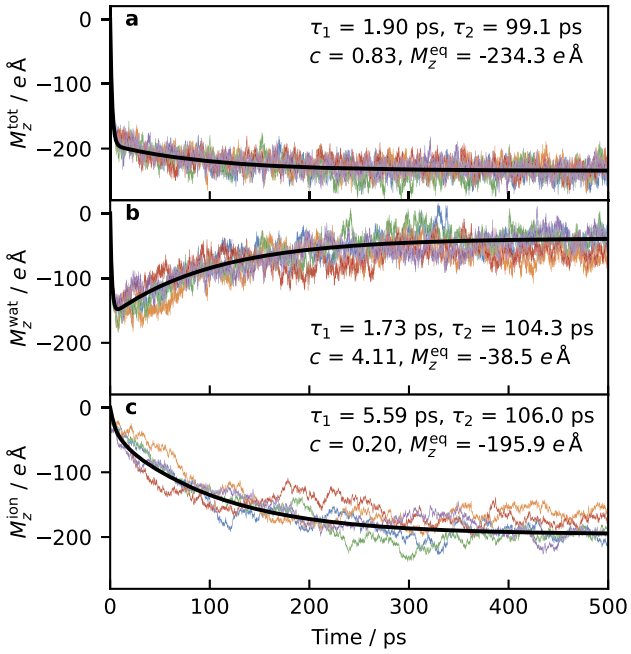

FIG. 1. Individual fitting parameters of the bi-exponential function [cf. Eq. (15)] applied to (a) the total dipole M_z^{tot}, (b) the dipole of water molecules M_z^{wat}, and (c) to the dipole of ions in the electrolyte M_z^{ion} from a standard CPM simulation at 2 V. While only five of the 100 trajectories are shown for illustration, fits are made to the entire set of trajectories.

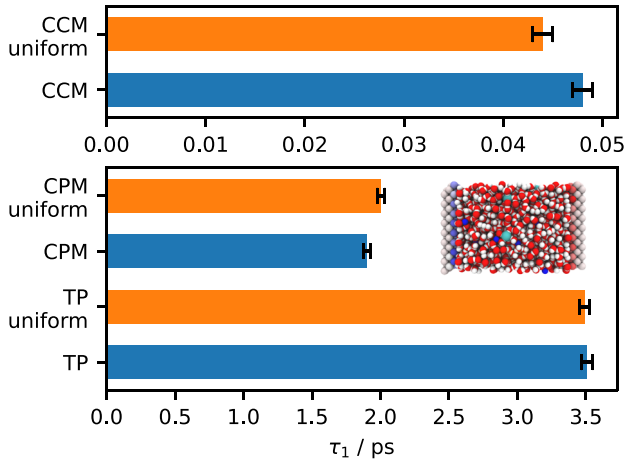

FIG. 2. Charging time constants τ_1 and empirical standard deviations employing different CPM approaches as denoted on the y axis. Inset shows the model system used to compare the different approaches, consisting of an aqueous NaCl electrolyte in contact with two gold surfaces. Note the different charging time constants τ_1 for the CCM and CPM approaches.

smaller than obtained with the potential-based methods, which is a well-known effect[6,55] that could be related to rather unphysical high temperatures and voltages when applying an instantaneous charge with CCM on the electrodes.[6] CCM also predicts two times smaller τ_2 than other methods, while the contribution of the second exponential decay is almost negligible since $c = 0.98$ in Eq. (15). However, these values should be interpreted with caution, given that the bi-exponential curve is a poor fit in the case of a CCM (cf. Fig. S2). Using the TP, little change in the slower timescale τ_2 is observed compared to the CPM and it only weakly depends on the time constant τ_ν (cf. Table S1). In contrast, the applied voltage ν_0 in a CPM has an effect on the ionic charging times τ_2, and for a smaller applied voltage of 0.3 V, τ_2 drops to 50 ps (cf. Fig. S4).

Using a TF model for representing real metals impacts both charging times and the total dipole. It is interesting to note that while a decrease for τ_1 with increasing l_{TF} in Fig. S3(a) is observed, interpretation of τ_2 is more complex when using a TF (cf. Table S1), especially when comparing this to a regular CPM, i.e., $l_{TF} = 0$, at the same voltage. The small difference between a regular CPM and the TF for small l_{TF} might be an artifact due to the rather thin metal slab model or might be due to a complex interplay between charge screening in the metal and the water/ionic relaxation and/or the smaller total dipole obtained with the TF model.

To understand the range of the second relaxation time $\tau_2 \approx 50$–100 ps, it is instructive to consider the product RC of the aforementioned areal capacitance $C = 2.94\ \mu\text{F cm}^{-2}$ and the areal electrolyte resistance R. Continuum models for ion dynamics have shown that the ionic relaxation time decently agrees with RC for applied potentials up to around the thermal voltage $k_BT/e \approx 25$ mV;[56,57] a recent dynamical density functional theory for a dense electrolyte found that the ions relaxed with RC even around 1 V.[58] In a bulk electrolyte at infinite dilution, the areal resistance between two electrodes spaced L apart is given by $R = L\rho$, where $\rho = k_BT/(2e^2Dc_b)$ is the ionic resistivity, k_BT is the thermal energy, e is the elementary charge, D is the ionic diffusion constant, and c_b is the salt number density.[59] In our simulations, the plate separation was $L = 5$ nm and the salinity in the bulk phase was ≈ 0.95M, corresponding to $c_b \approx 0.57\ \text{nm}^{-3}$; the ion diffusivity $D \approx 1.5 \cdot 10^{-9}\ \text{m}^2/\text{s}$ was obtained from a separate bulk electrolyte simulation. Using these values, we obtained $RC = 14$ ps, which is roughly seven times smaller than the largest fitted τ_2. This discrepancy must be due partly to our underestimation of ρ, which, at the salinity of our interest, is larger by a factor of about 1.7;[59] accounting for this effect yields a relaxation time of $RC = 23$ ps. Another cause of the remaining factor 4 discrepancy between the largest fitted τ_2 and predicted ionic relaxation times is the nanoconfinement, which could affect the diffusivity D and, in turn, the areal resistivity R. Finally, the mentioned increase of τ_2 with the applied potential is in line with the potential dependence of the capacitance of the Gouy–Chapman model, though in disagreement with that of the Kilic–Bazant–Ajdari[60] model. Although the analytical estimates of RC times presented here provide starting points for further research on the implications of nanoconfinement and finite salt concentration on charging times, these results should not be overinterpreted as the analytical models contain simplifications that may not apply to such nanoscopic systems.

B. Coaxial cylindrical capacitor

As a sanity check of our approach for systems that are periodic in just one dimension, we study the capacitance of two coaxial

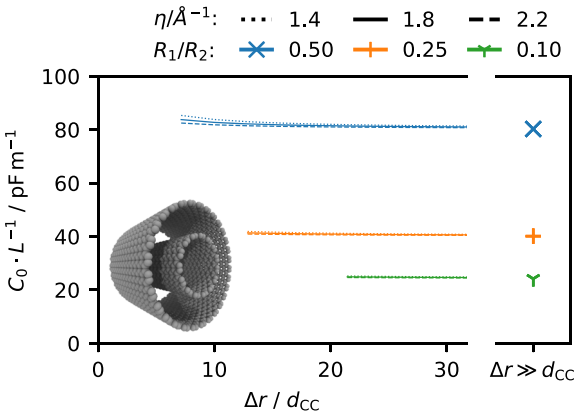

FIG. 3. Dielectric capacitance of cylindrical capacitors for fixed ratios of R_1/R_2 with R_1 the inner and R_2 the outer tube radii. Results for coaxial carbon nanotubes computed with MD are indicated as lines. Marks denote analytical results for a structureless equivalent system. The difference between the radii $\Delta r = R_2 - R_1$ is given relative to the characteristic bond length d_{CC} between carbon atoms in graphene.

carbon nanotubes of radii R_1 and R_2, with $R_1 < R_2$ (cf. inset of Fig. 3). The vacuum capacitance C_0 of the coaxial carbon nanotubes can be calculated from the electrode-wise capacitance $\tilde{\mathbf{C}}$.[34] At large radii, the atomic structure of the tubes should have a negligible effect, and thus the capacitance should approach that of structureless cylinders. The analytical line capacitance for a given ratio of the radii is $C_0/L = 2\pi\varepsilon_0/\ln(R_2/R_1)$, in which ε_0 is the vacuum permittivity and L is the length of the simulation box in the periodic dimension. As shown in Fig. 3 for various fixed ratios of the inner and outer tubes, the capacitance indeed converges to that of a structureless cylindrical capacitor when the radii are large compared to the bond length d_{CC} between carbon atoms. In the CPM, electrode atoms are assigned a Gaussian charge distribution $\rho_i(\mathbf{r}) = q_i\left(\eta^2/\pi\right)^{3/2} \exp\left[-\eta^2(\mathbf{r} - \mathbf{R}_i)^2\right]$ at their position $\mathbf{R}_i$ with the reciprocal charge width η. In agreement with Serva *et al.*,[61] increased capacitances are observed for larger Gaussian width (i.e., smaller η) in Fig. 3. However, the impact is almost negligible.

IV. CONCLUSIONS

We presented the ELECTRODE package as an efficient implementation of the constant potential method (CPM) and closely related methods for the popular LAMMPS simulation environment. Initially, the main goal was to bundle many different approaches to electrochemical simulations into one package and ensure that they are handled in the most computationally efficient way. However, we also found interesting relationships between the two relevant charging time contributions, i.e., water dipole relaxation and ion diffusion. We also implemented several new features, such as the EW2D summation and a correction for systems periodic in just one dimension, whose capabilities and full potential have been scarcely explored and which also work independently of the CPM. Recent improvements to the CPM, such as the finite field (FF) method and a Thomas–Fermi (TF) model, were included and compared for consistency to results found in the literature. Remarkably, using the TF model with varying TF lengths has a surprising and complex impact on the water and ionic relaxation times.

These results demonstrate that the ELECTRODE package can efficiently simulate electrified interfaces, including unusual systems such as infinitely long charged nanotubes. For a capacitor composed of coaxial carbon nanotubes, the vacuum capacitance agrees well within the limit of the analytical result of a structureless cylindrical capacitor and enables future investigations of curvature-dependent effects[24,57] more rigorously by avoiding interactions between the nanotubes through the periodic images. Moreover, the charging process of a plate capacitor with an aqueous NaCl electrolyte in-between vividly illustrates the differences between the range of methods introduced here and which are used to estimate the electrode charges. Interestingly, in these simulations, it was observed that the water dipole initially responds very quickly to the applied potential but then slowly drops off as the ionic dipole slowly builds up, as if the water dipoles were shielded from the ions.

While the package is in a stable state, its development is still ongoing and will include in the future features like a conjugate gradient solver or compatibility to TIP4P water models.

SUPPLEMENTARY MATERIAL

The supplementary material provides more background on the thermo-potentiostat (TP), boundary corrections, and the FF method. Furthermore, a description of the package interface to LAMMPS and an overview of the implemented classes are given. More details on the simulations are provided, including plots of trajectories and of charging times as a function of the voltage, the TF length, and the time constant of the TP.

ACKNOWLEDGMENTS

The authors acknowledge funding provided by the Deutsche Forschungsgemeinschaft (DFG, German Research Foundation)—Project Nos. 192346071 and 390794421—Grant Nos. SFB 986 and GRK 2462.

AUTHOR DECLARATIONS

Conflict of Interest

The authors have no conflicts to disclose.

Author Contributions

Ludwig J. V. Ahrens-Iwers: Conceptualization (equal); Formal analysis (supporting); Investigation (lead); Methodology (equal); Software (equal); Validation (equal); Writing – original draft (lead); Writing – review & editing (supporting). **Mathijs Janssen**: Conceptualization (supporting); Methodology (supporting); Validation (supporting); Writing – review & editing (supporting). **Shern R. Tee**: Conceptualization (equal); Formal analysis (equal); Investigation (equal); Methodology (equal); Resources (equal); Software (equal); Supervision (equal); Writing – original draft (equal); Writing – review & editing (equal). **Robert H. Meißner**: Conceptualization (equal); Data curation (equal); Formal analysis (equal);

Investigation (equal); Methodology (equal); Project administration (equal); Software (equal); Supervision (equal); Writing – original draft (equal); Writing – review & editing (equal).

DATA AVAILABILITY

The ELECTRODE package has been merged into the official release of LAMMPS which is available under https://github.com/lammps/lammps/tree/release.

REFERENCES

[1] C. Merlet, B. Rotenberg, P. A. Madden, and M. Salanne, Phys. Chem. Chem. Phys. **15**, 15781 (2013).
[2] K. Breitsprecher, K. Szuttor, and C. Holm, J. Phys. Chem. C **119**, 22445 (2015).
[3] J. Vatamanu, O. Borodin, and D. Bedrov, J. Chem. Theory Comput. **14**, 768 (2018).
[4] J. B. Haskins and J. W. Lawson, J. Chem. Phys. **144**, 184707 (2016).
[5] J. Gäding, G. Tocci, M. Busch, P. Huber, and R. H. Meißner, J. Chem. Phys. **156**, 064703 (2022).
[6] C. Merlet, C. Péan, B. Rotenberg, P. A. Madden, P. Simon, and M. Salanne, J. Phys. Chem. Lett. **4**, 264 (2013).
[7] J. I. Siepmann and M. Sprik, J. Chem. Phys. **102**, 511 (1995).
[8] S. K. Reed, O. J. Lanning, and P. A. Madden, J. Chem. Phys. **126**, 084704 (2007).
[9] S. Tyagi, M. Süzen, M. Sega, M. Barbosa, S. S. Kantorovich, and C. Holm, J. Chem. Phys. **132**, 154112 (2010).
[10] M. K. Petersen, R. Kumar, H. S. White, and G. A. Voth, J. Phys. Chem. C **116**, 4903 (2012).
[11] K. A. Dwelle and A. P. Willard, J. Phys. Chem. C **123**, 24095 (2019).
[12] T. D. Nguyen, H. Li, D. Bagchi, F. J. Solis, and M. Olvera de la Cruz, Comput. Phys. Commun. **241**, 80 (2019).
[13] K. Breitsprecher, M. Janssen, P. Srimuk, B. L. Mehdi, V. Presser, C. Holm, and S. Kondrat, Nat. Commun. **11**, 6085 (2020).
[14] S. Kondrat, P. Wu, R. Qiao, and A. A. Kornyshev, Nat. Mater. **13**, 387 (2014).
[15] S. Kondrat and A. A. Kornyshev, Nanoscale Horiz. **1**, 45 (2016).
[16] Z. Wang, Y. Yang, D. L. Olmsted, M. Asta, and B. B. Laird, J. Chem. Phys. **141**, 184102 (2014).
[17] D. T. Limmer, C. Merlet, M. Salanne, D. Chandler, P. A. Madden, R. Van Roij, and B. Rotenberg, Phys. Rev. Lett. **111**, 106102 (2013).
[18] C. Merlet, D. T. Limmer, M. Salanne, R. van Roij, P. A. Madden, D. Chandler, and B. Rotenberg, J. Phys. Chem. C **118**, 18291 (2014).
[19] C. Merlet, B. Rotenberg, P. A. Madden, P.-L. Taberna, P. Simon, Y. Gogotsi, and M. Salanne, Nat. Mater. **11**, 306 (2012).
[20] C. Merlet, C. Péan, B. Rotenberg, P. A. Madden, B. Daffos, P.-L. Taberna, P. Simon, and M. Salanne, Nat. Commun. **4**, 2701 (2013).
[21] E. H. Lahrar, P. Simon, and C. Merlet, J. Chem. Phys. **155**, 184703 (2021).
[22] A. C. Forse, C. Merlet, J. M. Griffin, and C. P. Grey, J. Am. Chem. Soc. **138**, 5731 (2016).
[23] J. Seebeck, P. Schiffels, S. Schweizer, J.-R. Hill, and R. H. Meißner, J. Phys. Chem. C **124**, 5515 (2020).
[24] J. Seebeck, C. Merlet, and R. H. Meißner, Phys. Rev. Lett. **128**, 086001 (2022).
[25] J. G. McDaniel, J. Phys. Chem. C **126**, 5822 (2022).
[26] D. L. Z. Caetano, S. J. de Carvalho, G. V. Bossa, and S. May, Phys. Rev. E **104**, 034609 (2021).
[27] A. P. Thompson, H. M. Aktulga, R. Berger, D. S. Bolintineanu, W. M. Brown, P. S. Crozier, P. J. in 't Veld, A. Kohlmeyer, S. G. Moore, T. D. Nguyen, R. Shan, M. J. Stevens, J. Tranchida, C. Trott, and S. J. Plimpton, Comput. Phys. Commun. **271**, 108171 (2022).
[28] L. J. V. Ahrens-Iwers and R. H. Meißner, J. Chem. Phys. **155**, 104104 (2021).
[29] F. Deißenbeck, C. Freysoldt, M. Todorova, J. Neugebauer, and S. Wippermann, Phys. Rev. Lett. **126**, 136803 (2021).
[30] L. Scalfi, T. Dufils, K. G. Reeves, B. Rotenberg, and M. Salanne, J. Chem. Phys. **153**, 174704 (2020).
[31] T. Dufils, G. Jeanmairet, B. Rotenberg, M. Sprik, and M. Salanne, Phys. Rev. Lett. **123**, 195501 (2019).
[32] T. Dufils, M. Sprik, and M. Salanne, J. Phys. Chem. Lett. **12**, 4357 (2021).
[33] S. R. Tee and D. J. Searles, J. Chem. Phys. **156**, 184101 (2022).
[34] L. Scalfi, D. T. Limmer, A. Coretti, S. Bonella, P. A. Madden, M. Salanne, and B. Rotenberg, Phys. Chem. Chem. Phys. **22**, 10480 (2020).
[35] J. Vatamanu, O. Borodin, and G. D. Smith, Phys. Chem. Chem. Phys. **12**, 170 (2010).
[36] H. Li, G. Jiang, P. Wang, and J. Z. Liu, "A simple and efficient lattice summation method for metallic electrodes in constant potential molecular dynamics simulation," arXiv:2111.06704 (2021).
[37] A. Coretti, L. Scalfi, C. Bacon, B. Rotenberg, R. Vuilleumier, G. Ciccotti, M. Salanne, and S. Bonella, J. Chem. Phys. **152**, 194701 (2020).
[38] Z. Hu, J. Chem. Theory Comput. **10**, 5254 (2014).
[39] A. Schlaich, D. Jin, L. Bocquet, and B. Coasne, Nat. Mater. **21**, 237 (2022).
[40] L. Scalfi, M. Salanne, and B. Rotenberg, Annu. Rev. Phys. Chem. **72**, 189 (2020).
[41] A. Marin-lafleche, "Ewald summation in 2D and 3D for a set of point charges and Gaussian charges," https://gitlab.com/ampere2/metalwalls/-/raw/release/doc/theory/ewald-summation/ewald.pdf, 2020.
[42] T. Gingrich, "Simulating surface charge effects in carbon nanotube templated ionic crystal growth," https://gingrich.chem.northwestern.edu/papers/ThesiswCorrections.pdf, 2010.
[43] G. Jeanmairet, B. Rotenberg, and M. Salanne, Chem. Rev. **122**, 10860 (2022).
[44] E. R. Smith, Proc. R. Soc. London, Ser. A **375**, 475 (1981).
[45] I.-C. Yeh and M. L. Berkowitz, J. Chem. Phys. **111**, 3155 (1999).
[46] S. W. De Leeuw and J. W. Perram, Mol. Phys. **37**, 1313 (1979).
[47] D. M. Heyes, M. Barber, and J. H. R. Clarke, J. Chem. Soc., Faraday Trans. 2 **73**, 1485 (1977).
[48] D. E. Parry, Surf. Sci. **49**, 433 (1975).
[49] A. Bródka and P. Śliwiński, J. Chem. Phys. **120**, 5518 (2004).
[50] A. Arnold, J. de Joannis, and C. Holm, J. Chem. Phys. **117**, 2496 (2002).
[51] J. de Joannis, A. Arnold, and C. Holm, J. Chem. Phys. **117**, 2503 (2002).
[52] A. Marin-Laflèche, M. Haefele, L. Scalfi, A. Coretti, T. Dufils, G. Jeanmairet, S. Reed, A. Serva, R. Berthin, C. Bacon, S. Bonella, B. Rotenberg, P. Madden, and M. Salanne, J. Open Source Software **5**, 2373 (2020).
[53] A. M. Sampaio, G. F. L. Pereira, M. Salanne, and L. J. A. Siqueira, Electrochim. Acta **364**, 137181 (2020).
[54] C. Noh and Y. Jung, Phys. Chem. Chem. Phys. **21**, 6790 (2019).
[55] J. Vatamanu, O. Borodin, and G. D. Smith, J. Phys. Chem. B **115**, 3073 (2011).
[56] M. Z. Bazant, K. Thornton, and A. Ajdari, Phys. Rev. E **70**, 021506 (2004).
[57] M. Janssen, Phys. Rev. E **100**, 042602 (2019).
[58] K. Ma, M. Janssen, C. Lian, and R. van Roij, J. Chem. Phys. **156**, 084101 (2022).
[59] Y. Avni, R. M. Adar, D. Andelman, and H. Orland, Phys. Rev. Lett. **128**, 098002 (2022).
[60] M. S. Kilic, M. Z. Bazant, and A. Ajdari, Phys. Rev. E **75**, 021502 (2007).
[61] A. Serva, L. Scalfi, B. Rotenberg, and M. Salanne, J. Chem. Phys. **155**, 044703 (2021); arXiv:2106.07232.